

## Compaction of DNA on nanoscale three-dimensional templates

This article has been downloaded from IOPscience. Please scroll down to see the full text article.

2006 J. Phys.: Condens. Matter 18 R453

(<http://iopscience.iop.org/0953-8984/18/28/R01>)

View [the table of contents for this issue](#), or go to the [journal homepage](#) for more

Download details:

IP Address: 129.252.86.83

The article was downloaded on 28/05/2010 at 12:17

Please note that [terms and conditions apply](#).

## TOPICAL REVIEW

# Compaction of DNA on nanoscale three-dimensional templates

Anatoly A Zinchenko and Ning Chen

Department of Physics, Graduate School of Science, Kyoto University, Kyoto 606-8502, Japan

E-mail: [zinchenko@chem.scphys.kyoto-u.ac.jp](mailto:zinchenko@chem.scphys.kyoto-u.ac.jp)

Received 16 February 2006

Published 28 June 2006

Online at [stacks.iop.org/JPhysCM/18/R453](http://stacks.iop.org/JPhysCM/18/R453)

## Abstract

There exist several important *in vivo* examples, where a DNA chain is compacted on interacting with nanoscale objects such as proteins, thereby forming complexes with a well defined molecular architecture. One of the well known manifestations of such a natural organization of a semi-flexible DNA chain on nanoscale objects is hierarchical DNA molecule assembly into a chromosome, which is mediated by cationic histone proteins at the first stages of compaction. The biological importance of this and other natural nanostructural organizations of the DNA molecule has inspired many theoretical and numerical studies to gain physical insight into this problem. On the other hand, the experimental model systems containing DNA and nanoobjects, which are important to extend our knowledge beyond natural systems, were almost unavailable until the last decade. Accelerating progress in nanoscale chemistry and materials science has brought about various nanoscale three-dimensional structures such as dendrimers, nanoparticles, and nanotubes, and thus has provided a basis for the next important step in creating novel DNA-containing nanostructures, modelling of natural DNA compaction, and verification of accumulated theoretical predictions on the interaction between DNA and nanoscale templates. This review is written to highlight this early stage of nano-inspired progress and it is focused on physico-chemical and biophysical experimental investigations as well as theoretical and numerical studies dedicated to the compaction of DNA on nanoscale three-dimensional templates.

(Some figures in this article are in colour only in the electronic version)

## Contents

1. Introduction	454
2. Multications, polyelectrolytes, cationic surfaces, and three-dimensional templates from the nanoworld for DNA compaction	455

3. Natural three-dimensional templates: gyrase, histone, and other proteins	457
4. Theoretical and numerical studies on DNA interaction with oppositely charged spherical macroions	461
5. DNA interaction with micelles, vesicles, and liposomes	465
6. Complexes between DNA and dendrimers	467
7. DNA compaction with nanoparticles	469
8. Theoretical and experimental studies on DNA interaction with nanotubes	474
9. Conclusions and perspectives	476
Acknowledgments	477
References	477

## 1. Introduction

The importance of the DNA compaction phenomenon is irrefutable, because in living organisms DNA is stored and functions in a compact form of various densities. In the most extreme cases, up to a hundred thousand times higher molecular density compared to the DNA unfolded form is achieved [1]. Two types of DNA compaction can be clearly distinguished in nature: compaction of long DNA chains with the help of multicationic species into extremely dense nanostructures realized in bacteriophages' heads [2], and compaction of DNA by nanoscale three-dimensional templates such as histones [3]. There also exist other examples of biological events when local concentrating of a DNA molecular chain near the surface of a protein is vital for a proper DNA biological functioning. These two types of DNA compaction have representative analogues in *in vitro* studies. DNA compaction by low molecular weight compaction agents such as spermidine and spermine mimics the dense packing of long DNA chains in a bacteriophage head. Less dense compaction of DNA chain on artificial nanoscale templates such as synthetic nanoparticles and nanotubes, prototyped by the DNA–histone complex, is nowadays much less studied and understood.

The term 'DNA compaction' has been reserved to describe condensing of a *single* DNA chain into compact condensates in contrast to the 'DNA condensation' phenomenon, where both single- and multi-molecular events in the processes of DNA condensed phase formation take place [8]. Furthermore, when we deal with nanoscale templates, the meaning of the term 'DNA compaction' becomes broader, and can also refer to the phenomena of DNA chain concentrating near the oppositely charged surface of a nanoscale object, i.e. the object whose geometry can play a certain role in the mechanism of DNA compaction and organization into condensate. The scientific interest in the DNA compaction phenomenon is two-fold. On the one hand, compaction of DNA has attracted significant attention of physicists as an example of a semi-flexible polyelectrolyte chain phase transition [4]. On the other hand, synthetic efforts to create chemical compounds for controllable DNA compaction are responsible for significant progress in gene delivery [5]. As a future goal, the elaboration of new approaches for the controllable assembly of a DNA chain on three-dimensional templates and understanding of the driving forces in such an assembly are expected to give a deeper insight into mimicking of biologically relevant organizations of a DNA chain in natural complexes. Controlling of the DNA conformational behaviour through a fine tune of physical parameters in systems containing a semi-flexible DNA chain is also expected to contribute to the creation of new DNA nanostructures with a programmable biological activity of the DNA chain.

This review is focused on the recent progress in theoretical and experimental studies on how a semi-flexible double-stranded DNA chain interacts with both biological and newly appeared synthetic nanoscale three-dimensional templates. Unless otherwise mentioned, only compaction of native double-stranded DNA molecules is described. Before we start the

discussion, we would like to mention earlier important reviews which are relevant to the topic. The review of Schiessel entitled 'The physics of chromatin' [3] describes in detail the physical basis and the state of science with respect to the problem of DNA interaction with histone proteins. The processes of DNA self-organization into compact condensates has been reviewed by Bloomfield [6] (DNA condensation); Hud [7] (morphology of DNA condensates), and Yoshikawa [8, 9] (single-molecule DNA compaction). The reviews of Joanny [10] and colleagues (adsorption of charged polymers), and Grosberg and colleagues (charge inversion phenomena accompanied DNA compaction on nanoscale templates) [11] are also recommended.

## **2. Multications, polyelectrolytes, cationic surfaces, and three-dimensional templates from the nanoworld for DNA compaction**

Double-stranded DNA is a semi-flexible negatively charged polyelectrolyte, having a Kuhn segment length of 106 nm and a linear charge density equal to one charge per 1.7 Å, and such a simple definition is responsible for its conformational behaviour and all the spectrum of nanostructures which can be potentially realized upon a DNA chain condensing in space. The semi-flexible nature of the DNA polymer chain makes it a very versatile scaffold which can be considered as rigid or flexible depending on the length of DNA chain and experimental conditions. DNA is a rigid 'stick' when the length of DNA is of the order of a hundred base pairs, while it is quite flexible when the length of DNA reaches hundreds of thousands of base pairs, as in bacteriophages. In aqueous solution, DNA adapts a coil (unfolded) conformation as a result of intrinsic rigidity (mechanical component) and repulsion between negatively charged segments (electrostatic component). With an addition of oppositely charged species, which are usually called 'compaction agents', DNA is compacted into condensates of various densities and morphologies depending on the chemical nature of compaction agent. All these DNA compaction agents can be classified into zero-dimensional (multivalent cations), one-dimensional (polycations with linear arrangement of charges), two-dimensional (cationic surfaces), and three-dimensional (nanostructures with a certain volume geometry). The following very basic features of DNA compaction by multications (zero-dimensional) are well known. A DNA chain in extended coil conformation undergoes compaction into an extremely compact condensate when the threshold of about 90% of DNA negative charges becomes neutralized by oppositely charged compaction agents [6, 12]. This compaction at the level of single DNA chains proceeds as an all-or-none type transition [8]. Thus formed compact DNA condensates represent toroid morphology [7]; less common morphologies are rod or globule [9]. In toroids, DNA chains are packed in a hexagonal lattice [13] where the DNA charge is neutralized and only the surface of the DNA condensate has a residual negative charge. One-dimensional compaction of DNA with polyelectrolytes becomes almost stoichiometric in terms of the ratio between DNA charges and charges of the polycation and in a majority of cases the toroidal shape of the DNA condensate is not preserved [9]. The all-or-none scenario changes into continuous DNA chain compaction.

The next level, two-dimensional compaction of DNA on charged surfaces, takes us closer to the understanding of the three-dimensional (3D) compaction realized on large nanoobjects, since a surface can be considered as a part of large 3D template. Many features found for DNA adsorption on charged surfaces were also observed in studies on DNA interaction with large spherical polycations such as vesicles or liposomes, and such features will be discussed in the corresponding section of this review. Three-dimensional DNA compaction is the next step in the hierarchy of DNA chain organization, which is mediated by supramolecular or colloid objects.

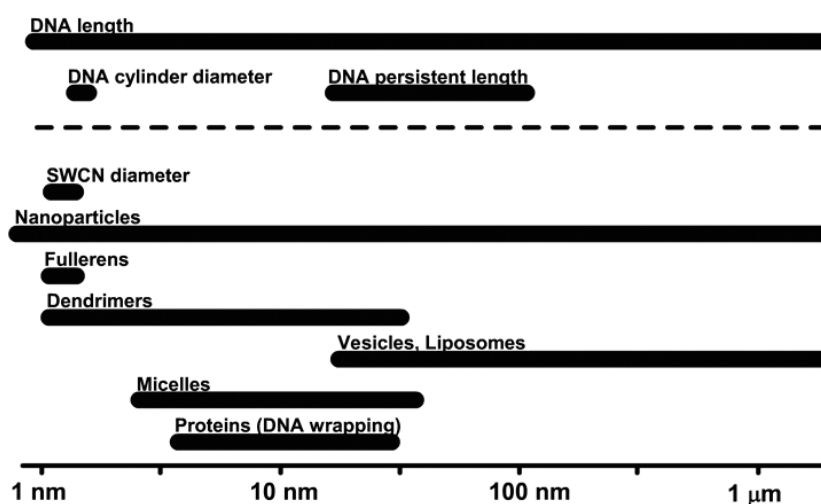


**Figure 1.** Approximate dimensions of nanoscale and submicroscale templates used for DNA compaction shown together with main geometrical parameters of double-stranded DNA. Compaction agents are arranged in the order of the appearance of studies on their interaction with DNA (from bottom to the top dash line).

The main classes of available nanoscale templates which may induce compaction of DNA are shown in figure 1, where natural and synthetic nanosized and microsized templates for DNA compaction are arranged according to their size. The vertical axis of this graph shows an appearance of studies on DNA interaction with corresponding nanostructures in time.

Natural nanoscale templates which fold a DNA chain are comprised of proteins with well defined architecture formed as a result of protein folding. Among these DNA-interacting proteins, histone proteins are probably the most important and, thus, the most studied representatives. DNA interacts with histone proteins by wrapping around each histone about two times. In the case of other proteins such as *lac* repressor [14], DNA gyrase [15], and UvrB [16], the DNA is concentrated near the protein surface (generally through significant bending) to allow for specific biological functions. Nevertheless, we also include such proteins in the group of natural nanoscale templates providing a local increase of DNA density through wrapping.

The number and versatility of existed artificial (synthetic) nanoscale templates for DNA compaction is considerably broader. Figure 1 shows currently available synthetic nanostructures and their characteristic sizes. The earliest studied nanoscale objects in relation to their interaction with DNA were micelles, vesicles and liposomes; these studies began in the early 1990s. Spherical branched polycations, dendrimers, became available about ten years ago. The dimension of these nanoscale templates was very similar to that of proteins operating with a DNA chain, and in particular, with histone proteins in nucleosomes. Being prepared by a stepwise organic grafting, dendrimers connect a molecular level (low generations) and nanoscale level over 10 nm (higher generations). A few years later, the first works on interaction between DNA and nanoparticles appeared; however, they mainly described large templates of submicron scales. Physico-chemical studies on DNA interaction with smaller nanoparticles appeared most recently. Finally, the youngest members in this group are nanoscale objects of elongated morphology such as nanotubes or dendronized polymers, which are still almost unexplored classes of potentially powerful DNA carriers. Nowadays,

nanoparticles and nanotubes in particular give many promises for future research, due to the possibility to vary their dimensions precisely but in a very broad range, which, for instance, was not possible in the case of dendrimers, micelles, etc.

In the same figure (figure 1), the fundamental geometrical parameters of a double-stranded DNA chain are shown: the diameter of the double-stranded DNA cylinder is about 2 nm, a persistent length—30–100 nm [17], which characterizes the rigidity of DNA, and the contour length of DNA chains that can achieve a centimetre order for a single DNA molecule. Therefore, DNA is a unique bridge between nano and micro ‘worlds’, having enormous potential for hierarchical nanoconstruction.

The semi-flexible and highly negatively charged nature of the DNA chain determines the interaction with nanoscale templates. Now it is well known that flexible polyelectrolytes such as polyacrylic acid or polystyrene sulfonate adsorb on cationic nanostructures freely, while rigid polyelectrolytes such as actin having a persistent length of several micrometres interact with nanostructures almost without changes in their own conformation. DNA flexibility lies between these two cases. Therefore, depending on the correlation between the size of the nanoscale objects and the rigidity of the DNA chain, both mechanisms of DNA interaction with nanoscale templates can be found upon DNA compaction: either DNA is freely adsorbed on large nanostructures or it collects small nanoobjects along its chain.

When the DNA chain is short, there is not much room left for nanoconstruction between DNA and nanoobjects, because DNA behaves as a rigid ‘stick’. The persistent length of DNA can vary in a range 30–100 nm and this means that in order to discuss DNA compaction at a single-molecule level, at least several hundred nanometre DNA chains should be considered for actual experiments. The organization of a DNA chain on three-dimensional templates is very versatile and can be subdivided into several separate issues. The first one is the possibility of DNA wrapping around the nanoscale object, which is much smaller than the persistent length of DNA. The second issue is the organization of the DNA chain on larger nanoparticle surfaces, i.e. the mutual arrangement of DNA chain cylinders. The third problem, which concerns only long DNA chains, is the way in which DNA complexed with nanoparticles is further organized into higher-order structures after interaction with nanoscale objects.

### 3. Natural three-dimensional templates: gyrase, histone, and other proteins

We begin our discussion with natural nanoscale templates that assist in the DNA compaction. As shown in figure 1, natural proteins are usually relatively small nanoscale templates of the order of 10 nm. DNA-interacting proteins generally bear an excess of positive charge, which is necessary to induce wrapping of the negatively charged DNA cylinder. The organization of DNA on the surface of proteins is critical for many DNA biological functions, including replication, transcription, recombination and repair, as well as the packaging and storage of chromosomal DNA. In the review by Saecker and Record [18], the authors discuss the generality of DNA wrapping organization with proteins and structural and thermodynamic signatures of DNA wrapping. They suggest that proteins wrapping up DNA should possess not only a large number of cationic side chains in the wrapping interface, but also they should have a significant number of anionic side chains further away from the DNA phosphates and in the vicinity of this interface. In addition, many cationic (lysine, arginine and histidine) groups on the protein surface that form hydrated ion pairs ( $\sim 4\text{--}6$  Å charge separation) with DNA phosphates in the wrapped complex can form dehydrated surface salt bridges ( $\sim 3$  Å charge separation) with neighbouring anionic (glutamate and aspartate) side chains in the free protein. Disruption of many of these protein salt bridges is required to create the cationic surface complementary to anionic DNA phosphates in the wrapped complex interface.

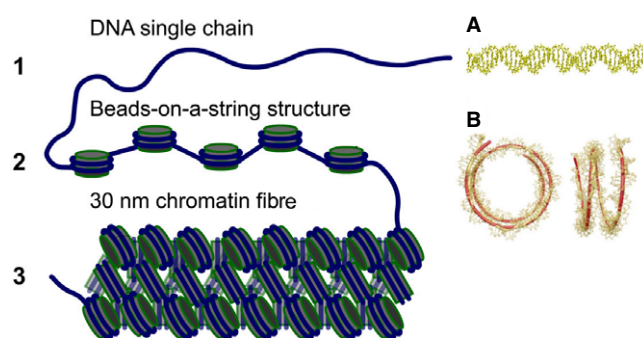


**Figure 2.** Schematic presentation of the first levels of DNA chain (1) packing into a chromosome through the formation of complexes with histones (grey cylinders), which are called 'beads-on-a-string' structures (2) and further organization into a 30 nm fibre of closed chromatin (3). At the right, the double-stranded structure of a DNA helix (A) is shown together with the fragment of DNA which wraps around one histone in a 'beads-on-a-string' structure (B) as was observed by x-ray diffraction studies. The fragment of DNA-wrapped histone (B) is reproduced with permission from Richmond and Davey [134]. Copyright 2003 Nature Publishing Group.

Experimental data about DNA complexation with histones and further organization into fibres are now very extensive and different aspects of this natural organization have been well reviewed [3]. Therefore, here we give only the essence of the existing knowledge and highlight the most recent findings. It has been already known for decades that the DNA in eukaryotic cells is compacted into a chromatin, which is a complex between DNA and small, highly basic proteins called histones [19–22]. The organization of a DNA chain into chromatin is multilevel and hierarchical; the first stages of this scenario of DNA assembling starting from a single DNA chain into a 30 nm fibre of chromatin are shown in figure 2.

The fundamental unit of chromosomal DNA packing in eukaryotes is the nucleosome [23, 24]. In the nucleosome, a portion of the DNA strand (147 bp, about 50 nm length) wraps approximately 1.75 times around a histone octamer (figures 2(B) and 4(A)) made from eight histone proteins (two copies each of core histone H2A, H2B, H3, and H4) [25–27], thus forming a nucleosome core particle. This basic repeating unit of the chromatin structure is now well characterized [25, 28–31]. The x-ray structure of the core nucleosome particle demonstrates that wrapping is nonspecific binding of DNA (deformable or, in some cases, initially bent) on a protein surface [25]. All interactions are with the DNA phosphodiester backbone, including more than 60 contacts between anionic phosphate oxygens and positively charged side chains of histones.

The nucleosomal core particles have a net negative charge because the negative charge of the wrapped DNA is significantly larger than the total positive charge of the histone protein octamer [32]. Based on an analysis of the salt dependence of nucleosomal DNA denaturation, it was estimated that only about 15% of the DNA phosphates participate in charge–charge interactions with histones [32].

Wrapping around the histone octamer, DNA forms nucleosomes, which in the case of long DNA chains form a 'beads-on-a-string' structure or so-called 10 nm chromatin fibre, characterized by a periodic arrangement of nucleosome core particles along the DNA strand (figure 2(2)) [33]. A string of nucleosomes participates in the next higher order level of DNA packing by folding into the 30 nm fibre [34] (figure 2(3)). Two basic models of 30 nm fibre organizations have been proposed: an earlier solenoid model [35] and later zig-zag crossed linker model [36]; however, at least six different models can be recognized with different



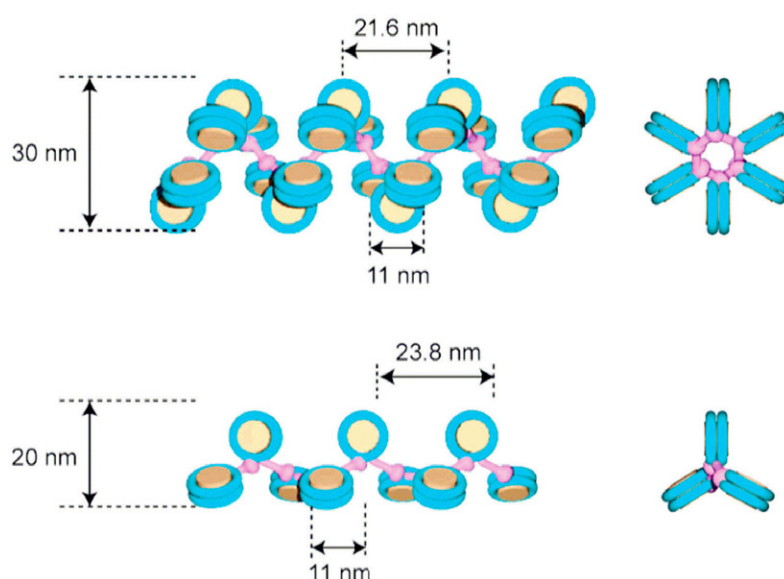


**Figure 3.** Models of nucleosome arrangement in the 30 nm fibre (top) and the 20 nm fibre (bottom). The upper structure is the so-called solenoid model of packaging. Reproduced with permission from Hizume *et al* [40]. Copyright 2005 American Chemical Society.

structural variations of nucleosome arrangement in the fibre [37]. Linker histones (H1), highly cationic polypeptides, play an important role in the formation of the 30 nm fibre form ‘beads-on-a-string’ structure. Removal of linker histones results in unfolding of the thicker fibre back into the ‘beads-on-a-string’ fibre [38, 33]. The 30 nm chromatin fibre provides about 40-fold linear compaction of naked DNA and it is characterized by a 200 nm persistent length [39] and a gyration radius about 20  $\mu\text{m}$ .

Further detailed studies on closed (30 nm) chromatin fibre formation showed that the width of the fibre depends on the ionic strength (figure 3) [40]. Widths of 20 nm in 50 mM NaCl became 30 nm as the ionic strength was changed to 100 mM. The authors proposed a flexible model of chromatin fibre formation, where the mode of the fibre compaction changes depending both on the salt environment and the presence of linker histone H1.

By observing reconstituted fibres of chromatin at different concentrations of histones, it was found that the density of nucleosomes exhibits a bimodal profile, i.e., there is a large transition between the dense and dispersed states in reconstituted chromatin [41]. This enables us to interpret the folding transition of reconstituted chromatin in terms of a first-order phase transition.

Attempts to mechanically stretch chromatin fibres provided an important insight into the forces responsible for chromatin fibre organization. The initial trials were made to use atomic force microscopy (AFM) to stretch both isolated native fibres and reconstituted nucleosomal arrays [42]. The force extension curves were found to have a multi-peak, saw-tooth pattern as a result of consecutive disassembly of individual nucleosomes in the fibre: the unravelling of the DNA from around each histone octamer was expected to lengthen the fibre in a jump and be accompanied by an abrupt drop in the force [43, 44]. For more details on the single molecule force measurements of chromatin fibres, the review of Zlatanova and Leuba is recommended [45].



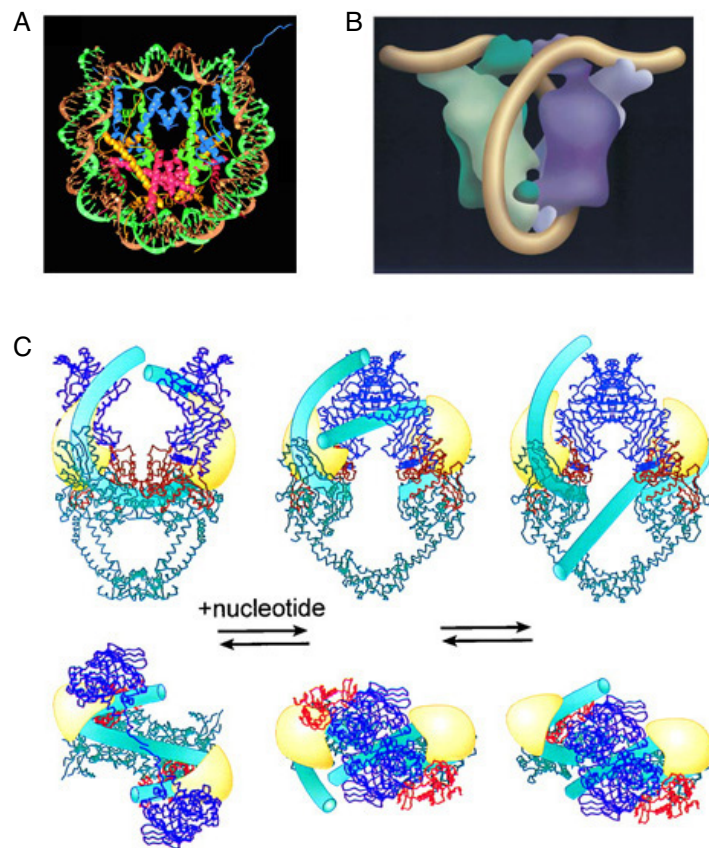


**Figure 4.** Structural models for the wrapping of double-stranded DNA on protein surfaces. (A) The x-ray structure of the core nucleosome particle demonstrates that wrapping is fundamentally nonspecific binding of DNA (deformable or, in some cases, initially bent) on a protein surface. (B) Model of DNA wrapping proposed for *lac* repressor, based on the crystal structure of LacI and on thermodynamic studies. (C) A model for the organization of the gyrase tetramer and the mechanism of DNA strand passage. DNA gyrase directs ~130 bp of DNA in a positive supercoil, whereas *lac* repressor (~120 bp) and the histone octamer (146 bp) wrap DNA in a negative supercoil. Reproduced with permission from Luger *et al* [25] (Copyright 1997 Nature Publishing Group), Tsodikov *et al* [14] (Copyright 1999 Elsevier) and from Kampranis *et al* [15] (Copyright 1999 National Academy of Science).

When DNA is wrapped onto the histones, it is 'silent', i.e. not accessible for DNA binding proteins. However, thermal fluctuations provide the opportunity for such proteins to interact with DNA via the unwrapping of either one of the two DNA turns [46, 47], or via a sliding of the histone octamer along the DNA chain [48, 49]. It was also shown that remodelling complexes can actively induce nucleosome sliding along DNA [50]. These phenomena provide access of other proteins to the DNA chain for copying genetic information. The possibility of unwrapping and sliding is controlled by H1 linker histone interaction [51]; as a result, the complexation of H1 histone leading to the formation of chromatin fibres constrains DNA genes into 'silence'.

DNA compacted into chromatin is not the only natural system in which DNA wraps proteins. In cells, a variety of DNA binding proteins regulates changes in DNA conformation

through the formation of specific nucleoprotein complexes, the most typical examples of which are presented in figure 4. DNA gyrase (figure 4(C)) is a molecular template that uses the energy of ATP (adenosine triphosphate) hydrolysis to introduce essential negative supercoils into DNA [52]. The structure of gyrase is a heart-shaped dimer with a central cavity and it has two interfaces, known as the DNA gate and the exit gate. The direction of such supercoiling is ensured by chiral wrapping of the DNA [53] around a specific domain. DNA makes a 30–37 nm wrap (90–112 bp) which was also demonstrated by electron microscope measurements of gyrase–DNA complexes [54]. This wrapping pass can be compared with the size of gyrase estimated from a variety of methods, which was found to be 20 nm [55], suggesting that the length of the wrapped DNA is significant with respect to the size of the protein. Wrapping of DNA around gyrase involves a large change in the end-to-end extension of the DNA [56]. Another protein which induces local DNA wrapping is *Lac* repressor shown in figure 4(B). In this long-lived complex, DNA interacting with the positively charged protein template makes one left-handed loop [14].

#### 4. Theoretical and numerical studies on DNA interaction with oppositely charged spherical macroions

Starting from the end of 1990s, a large number of theoretical works have been published that are dedicated to the interaction between polyanions, including DNA, and spherical polycations. In the majority of these reports, the interaction of one spherical polycation with a part of the polymer chain has been studied, and a few reports considered multi-particle interaction with DNA. All these studies can be further classified based on the flexibility of the polymer chain (flexible or semi-flexible) and the charge on the nanoparticles (highly or weakly charged). An additional distinction is based on high or low electrostatic screening conditions (concentration of low-molecular salt in solution).

Since the majority of theoretical studies and simulations have been dedicated to DNA interaction with histone proteins *in vivo*, the interaction between a semi-flexible chain and nanoscale spherical polycations has attracted particular attention. The main issues discussed in these theoretical studies are (i) conditions to realize different scenarios of DNA–nanoscale template interaction (e.g. wrapping, touching, etc), (ii) charge effects (overcharging and undercharging of DNA–macroion complexes), and (iii) local arrangement of a DNA chain on a nanoscale template surface. A number of different theoretical models have been proposed for DNA–histone complexes; among them, the first group of models focused on the geometry of the particle and DNA, characterized by a few parameters such as entry and exit angles [36, 57–60], while the other models focused on the electrostatic interactions between the charged spheres and equilibrated the structure of a single sphere/polyelectrolyte complex [61, 62].

Netz and Joanny introduced three states of interaction between a polyelectrolyte and a charged nanosphere: point touching, adsorption of a finite length of DNA on the nanosphere surface, and full wrapping [63]. Using a perturbation approach, they found conditions for the touching and wrapping transition of flexible and rigid polyelectrolytes around small and large nanospheres. Phase diagrams resulting from their theory for flexible and rigid polyelectrolytes are shown in figure 5. According to their theory, for intermediate salt concentration and high enough sphere charge, a stable DNA–nanosphere complex is formed in which the polymer completely wraps around the sphere. In the same study, conditions of the adsorption–desorption transition have been analysed. Later, Kunze and Netz studied semi-flexible chain complexation with one oppositely charged sphere using parameters similar to the real case of the DNA–histone complex by the linear Debye–Hückel approximation [64]. They also established phase diagrams with respect to sphere charge and salt concentration. The phase diagram presented in

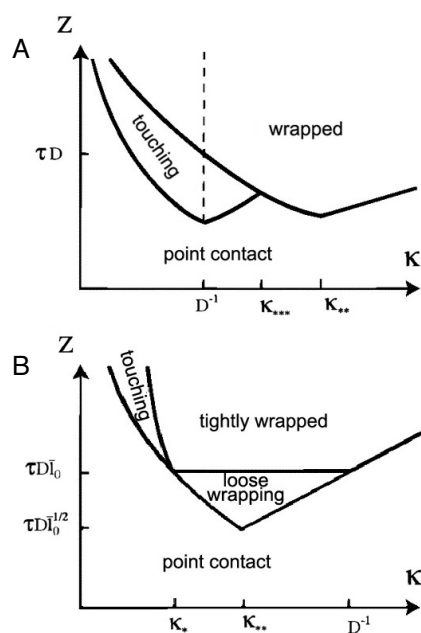


**Figure 5.** (A) Complete complexation phase diagram for a chain with a small bare bending rigidity as a function of the sphere charge  $Z$  and the inverse screening length. The touching transition, where the polymer starts touching the sphere over a finite contour length, and the wrapping transition, where the polymer completely wraps the sphere, are shown. The wrapping transition is strongly discontinuous when it goes directly from a point-contact phase to the wrapped phase, i.e., for high salt concentrations. The dotted line separates the hump from the bent configurations. (B) Complete complexation phase diagram for large bare bending rigidity. In contrast to figure 4, the touching phase is only observed for extremely low salt concentrations, and in addition, we observe a loosely wrapped phase, where the radius of the wrapping polymer is larger than the sphere radius. Reproduced with permission from Netz and Joanny [63]. Copyright 1999 American Chemical Society.

figure 6 shows that four different symmetry states of DNA complexation with a sphere exist, and that the wrapping transition of DNA around a nanosphere has a discontinuous nature. This salt dependence shows a great similarity to the behaviour of the natural DNA–histone system.

Studies on the statics and dynamics of the unwrapping process of a polyelectrolyte chain from a complex with spherical polycation [65] have also shown that the wrapping transition is a discontinuous process for a stiff chain. The complex between a flexible chain and a nanosphere is disordered, while for a stiff chain the complex structure is ordered, where there is a clear winding number, and the unwrapping process under external stretching is discontinuous with jumps of the distance–force curve. Brownian dynamics simulations showed that, even when a nanosphere is bound to a polyelectrolyte such as DNA with energy of tens of  $k_B T$ , the sliding motion along the chain is left as a surviving freedom in the nucleosome-like structure [66].

Besides the wrapped, partially wrapped and unwrapped structures introduced by Netz, a spectrum of multi-loop complexes, or ‘rosettes’, was predicted (see illustrations on figure 7). Systematic study on such multi-leafed states of DNA–nanosphere complexes was performed in the works of Schiessel and colleagues [67, 68] and also observed in computer simulations [69]. Such rosette structures were predicted for physiological and higher salt concentrations, where the electrostatic interaction is short-ranged, but it is expected that such structures can also be found at low salt concentrations, especially when the polyelectrolyte chain is rigid (highly

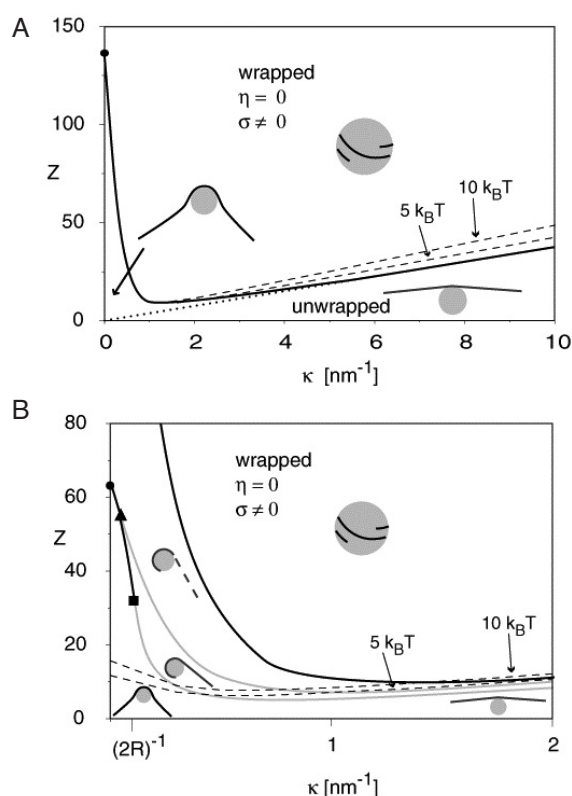


**Figure 6.** Phase diagram for a DNA strand of length  $L=550$  nm as a function of sphere charge  $Z$  and inverse screening length  $k$ . (A) The solid line indicates the transition from the wrapped state (phase I) to the 3D asymmetric state (phase II). The dotted line is a local-energy-balance argument for this wrapping transition, valid for large salt concentrations. The minimal sphere charge to wrap the DNA occurs at a screening length  $k^{-1} = 1$  nm, roughly corresponding to physiological salt condition. (B) Detail of the phase diagram for small  $k$ , featuring all four different phases. Discontinuous (continuous) transitions are denoted by black grey solid lines. The dashed lines indicate a complexation energy of  $5 k_B T$  and  $10 k_B T$ . Reproduced with permission from Kunze and Netz [135]. Copyright 2000 American Physics Society.

charged) and the particle is small. Figure 7 shows a diagram of DNA–nanosphere states under conditions of high salt. Interestingly, the transition between the ‘usual’ wrapping state and the rosette state (unwrapping transition) was found to be a sharp transition in the situation of short-range interactions [67]; in contrast, at low salt concentrations, this transition is smooth.

An interesting investigation has been dedicated to revealing the role of chirality of the nucleosome [70]. It was shown that the chirality of a nucleosome is strongly dependent on that of the histone octamer, and different chiralities of the histone octamer induce its different rotation directions in the wrapping process of DNA. Even a very weak chirality of the histone octamer is enough to induce the corresponding direction of DNA wrapping. This effect may be broken at elevated temperature.

While the situation with the first level of organization of DNA into ‘beads-on-a-string’ structure (figure 2(2)) is well studied experimentally and theoretically, and nowadays is relatively clear, the second level of such structural organization into a more dense fibre (figure 2(3)) is poorly understood. Therefore, most recent theoretical studies have been

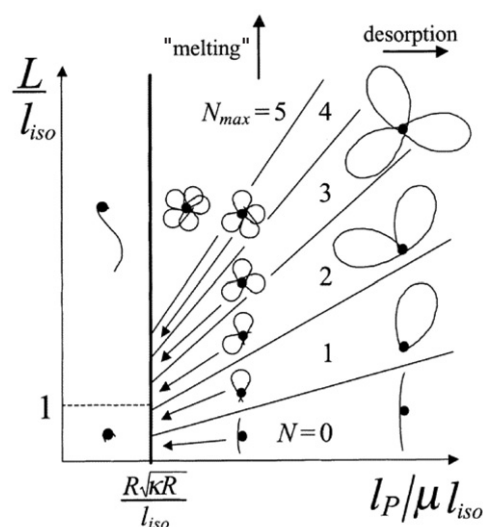


**Figure 7.** The sphere–chain complex in the case of short-range attraction (for instance, at high ionic strength). Depicted is the diagram of states as a function of the total length  $L$  of the chain and its persistence length  $l_p$  divided by the point contact energy  $\mu$  (both axes are in units of  $l_{iso}$ ). The thick vertical line indicates the sharp unwrapping transition from the wrapped to the rosette-type complexes. Reproduced with permission from Schiessel [67]. Copyright 2003 American Chemical Society.

dedicated to the formation of a fibre from the ‘beads-on-a-string’ structure and in particular to the mechanism of nucleosome attraction. Attraction between simplified model nucleosomes has been observed when the nucleosome particle has been mimicked by a cylinder with 277 charge patches [62], when the nucleosome was modelled by a negatively charged sphere wrapped around by a semi-flexible cationic chain [71], and when the histone tail-bridging effect was considered [72]. Most recently Netz continued developing the model of DNA–nanosphere complexation and analysed the system containing two cationic nanospheres complexed with DNA fragments [73]. It was shown that chain–sphere complexes can become highly coupled at small separations. In these regimes, polyelectrolyte chains on different spheres adapt their orientation and conformation in such a way that opposite charges from different complexes face each other. This leads to short-range attraction forces despite the fact that individual spheres are highly overcharged by the polyanion.

Considerable efforts have been made by different research groups to study charge effects during DNA complexation with oppositely charged nanoparticles and, in particular, to give an explanation of the counterintuitive overcharging phenomenon [74–81]. Evidence for the overcharging of charged macroions and surfaces by electrostatic interaction with oppositely charged macromolecules has been numerous demonstrated by many experimental studies (see the corresponding sections in this review for details). Both calculations without counterions in salt free solutions [74, 75, 124] and in the presence of salt [124] showed overcharging of the nanosphere macroion with adsorbed both strongly and weakly charged polyelectrolytes. When systems containing counterions were studied, it was shown that overcharging of the nanosphere is driven by the release of counterions upon polyelectrolyte chain adsorption on the nanosphere [82, 77].

Of particular interest is the extent of overcharging. In the above-mentioned model of Kunze and Netz [64], it was predicted that the model of a histone octamer can wrap a bendable line

model of DNA at physiological salt conditions using only 10 positive charges against the 300 negative charges on the DNA, which provides just 3% of charge neutralization. In a later work of Manning, the effect of counterion condensation was taken into account and it was found that the minimum amount of free energy required to bend DNA into axial conformity with the superhelical ramp at physiological salt concentration can be provided by a scant 6% neutralization of DNA phosphate charge [83].

Nguyen and Shklovskii [75, 76] emphasized the importance of correlation effects in the processes accompanied with a charge inversion and estimated that the inversion of charge (overcharging of sphere by DNA) can exceed 100%. This effect is manifested due to neighbouring turns of DNA on nanoscale templates repelling each other and forming an almost equidistant solenoid, which locally resembles a strongly correlated liquid. The tail of the polyelectrolyte repels the already adsorbed part of the polyelectrolyte and creates a correlation hole, which attracts the tail back to the surface. As a result, the net charge of the sphere with wrapped polyelectrolyte becomes negatively charged. They also predict the opposite situation, undercharging, when the number of nanospheres interacting with a chain is large. On this occasion, it should be noted that although the overcharging effect is always introduced as a general phenomenon in polyelectrolyte adsorption on nanospheres, this overcharging is realized at certain optimal conditions of complexation; therefore, overcharged complexes turned out to be undercharged when such parameters as polyelectrolyte rigidity, number of nanospheres per chain or concentration of monovalent salt in solution are changed.

Monte Carlo studies on the complexation between polyelectrolytes and spherical polycations have been performed for various chain models and for different subsets of parameter values [84–89], which demonstrated that in excess of spherical macroions the polyelectrolyte becomes consistently overcharged. Monte Carlo simulations by Linse and Jonsson demonstrated 50%–70% overcharging, where the larger value corresponds to the most rigid chain [87, 88].

## 5. DNA interaction with micelles, vesicles, and liposomes

These nanoscale objects are formed as a result of self-assembly of amphiphilic molecules driven by hydrophobic interactions between non-polar fragments of them. As it is seen in figure 1, the size of micelles is comparable to the thickness of the DNA chain (several nanometres), while vesicles and liposomes are larger and their size can reach the order of micrometres. Therefore, studies on DNA interaction with the representatives in this group of nanoscale templates focus on different aspects of such interaction depending on the nanoscale object size. As a result of the correlations between the DNA rigidity and the dimension of the nanoscale templates, DNA interaction with micelles is mainly discussed in terms of possibility of DNA wrapping around the micelle, while in case of larger liposomes and vesicles, the arrangement of the DNA chain on the charged surfaces of such self-assembled structures is discussed.

Earliest reports on DNA interaction with nanoscale spherical polycations are from Dubin and colleagues, who studied the interaction between DNA and positively charged micelles. They found that such interaction proceeds abruptly and the critical surface charge density of the micelle depends as a square root on the ionic strength of the solution. The same effect was also found when a positively charge polyelectrolyte interacts with negatively charged micelles [90, 91]. Plasmid DNA complexation with micelles with a mean diameter of 5 nm revealed three domains, depending on the DNA to micelle ratio [96]. These domains correspond to negatively charged, neutral, and positively charged complexes, respectively.

Vesicles are basically larger than micelles and typically have a size of several hundreds of nanometres, although the full range is from tens of nanometres to several micrometres. If the



case of micelle DNA interaction with spherical polycations is described in terms of assembling of micelles on a DNA chain, in the case of vesicles, such interaction is described as adsorption of the DNA chain on the vesicle surface. For example, it has been shown that DNA is adsorbed on vesicle surfaces (about 65 nm) and induces structural transitions in them [92]. Therefore, DNA molecules adapt to the template provided by the lipid self-assembled structure and not vice versa.

Although the adsorption of DNA on cationic bilayers is actually a two-dimensional event, the understanding of this DNA chain organization is related to the arrangement of the DNA chain on the surface of large nanoscale sub-microscale templates. On cationic bilayers, which are in the gel phase at room temperature, DNA forms a well-known highly ordered two-dimensional smectic phase with a regular spacing of several nanometres between adjacent DNA strands depending on the charge of the bilayer [93]. If the surface charge density is very high (purely cationic bilayers), the interaxial distance in the thereby formed DNA lattice is 6.5 nm, but when the charge of the lipid bilayer is reduced by 50%, the density of the adsorbed DNA decreases by 50% and the spacing between adjacent strands of DNA doubles to 13.0. Figure 8 illustrates this difference in DNA chain organization depending on the charge of the surface. It was also shown that with the addition of a divalent cation such as  $Mg^{2+}$  the interhelical distance between DNA chains adsorbed on a lipid bilayer decreases from about 5 to 3.5 nm, and has a minimum at concentration of dication about 0.5 M [94]. Moreover, DNA adsorbed on a two-dimensional lipid bilayer can be strongly condensed by the addition of divalent electrolyte counterions [95]. In striking contrast to bulk behaviour, synchrotron x-ray diffraction and optical absorption experiments showed that above a critical divalent counterion concentration the electrostatic forces between DNA chains adsorbed on surfaces of cationic membranes reverse from repulsive to attractive, and this leads to a chain collapse transition into a condensed phase of DNA tethered by divalent counterions. This demonstrates the importance of spatial dimensionality to intermolecular interactions, where nonspecific counterion-induced electrostatic attractions between like-charged polyelectrolytes overwhelm the electrostatic repulsions on a surface. Such a new phase, with a one-dimensional counterion liquid trapped between DNA chains at a density of 0.63 counterions per DNA bp, represents the most compact state of DNA on a surface *in vitro*.

The three-dimensional arrangement of DNA and lipids in their complexes called lipoplexes has also been studied. Structures of DNA complexes with different cationic lipid formulations were found to consist of a multi-lamellar lipid membrane in which DNA is intercalated [96–100]. A periodicity between DNA chains of 8 nm was observed when small spherical micelles about 5 nm in diameter were used, whereas a spacing of 6.5 nm was reported for the lamellar lipoplexes. These studies suggested that DNA was entrapped in condensed structures formed by means of interrelated lipid fusion and DNA collapse [101]. In addition to the lamellar phase, an inverted hexagonal columnar phase with DNA inside lipid tubes has been constructed through reduction of the membrane bending rigidity by adding low-molecular-weight helper molecules or induction of negative spontaneous membrane curvature by adding a zwitterionic lipid with cone-like molecular shape [102]. Both lamellar and hexagonal phases yield ordered DNA arrays, and through binding inorganic substances on the DNA chains [103], for instance, these structures serve as the templates to produce spatially ordered nanowires.

DNA is packed more tightly in negatively charged complexes than in isoelectric complexes; on the other hand, positively charged complexes have a lower packing density [100]. Therefore, overcharging of the complex away from its isoelectric point is caused by changes of the bulk structure with absorption of excess DNA on the cationic lipid. The degree of overcharging is dependent on the membrane charge density. Importantly, overcharged complexes are observed to move towards their isoelectric charge-neutral point at



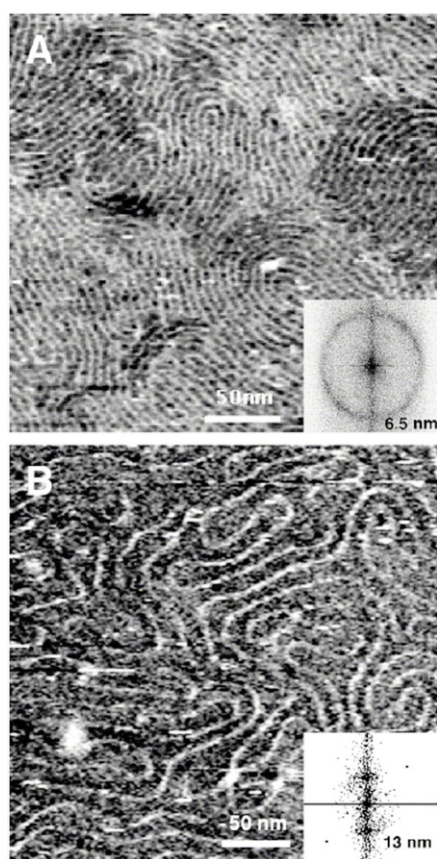


**Figure 8.** (A) DNA adsorbed on a supported DPTAP (dipalmitoyltrimethylammoniumpropane) bilayer. The DNA forms the well-known two dimensional smectic phase with a regular spacing of about 6.5 nm between adjacent DNA strands. (B) On a supported lipid bilayer of a 1:1 binary mixture of DPTAP and DPPC (dipalmitoyl-phosphatidylcholine), the spacing between adjacent strands of DNA doubles to about 13.0 nm. The height difference between DNA and lipids is 1.7 nm. Reproduced with permission from Clausen-Schaumann and Gaub [93]. Copyright 1999 American Chemical Society.

higher concentration of salt, with positively overcharged complexes expelling cationic lipid and negatively overcharged complexes expelling DNA.

## 6. Complexes between DNA and dendrimers

Dendrimers are a revolutionary class of organic molecules synthesized in a step-wise manner [104]. Dendrimers used for DNA studies are generally spherical polycations, which are named according to the number of successive graftings of their 'corona', starting from G0—initial precursor, G1—first modification, G2—second modification, etc; therefore, we have a series of charged spherical polycations with sizes from about 1 up to 10 nm in diameter. With the increase in generation number, the dendrimer molecules become larger but more dense; thereby their conformation changes from a soft sphere at middle generations (G4 to G8) to a hard sphere at high generations (>G8).

Two distinct mechanisms are expected for DNA interaction with dendrimers: DNA wrapping around a dendrimer, and dendrimers collecting on a DNA chain. First investigations



DNA/dendrimer loading ratio and dendrimer generation. Earlier observations [108] showed that circular DNA is complexed and compacted by G4 dendrimers into toroidal condensates; plasmid DNA is compacted with G7 dendrimer into toroidal structures and a fraction of irregular aggregates; while complexes of DNA with large G10 dendrimers were found mainly in the form of aggregates as lattice-like structures. This tendency was confirmed later by systematic AFM observations [109]. DNA was compacted by lower dendrimer generations (G4) into various morphologies: globules, toroids, rods, and ‘flowers’ (cf ‘rosettes’ of Schiessel) of comparable percentages. DNA condensates with G6 generation dendrimers were toroids and globules having usual dimensions of 50–100 nm, which were also observed in another study [110]. The population of globular DNA–G6 condensates was significantly larger compared to the observations of DNA–G4 complexes. Finally, G8 dendrimers condense DNA exclusively into globular morphology. Such a dependence of DNA condensate morphology on dendrimer generation is generally expected and it illustrates the change in the mechanism of DNA compaction from like-charge attraction, where low generation dendrimer molecules play the role of environmental parameter, to electrostatically driven adsorption of DNA chain on oppositely charged nanospheres. Taking into account the manifestation of the wrapping scenario in DNA–dendrimer complexation starting from the G7 generation of dendrimer, the disappearance of the toroidal shape of DNA condensates is attributed to the fact that DNA begins to wrap the dendrimer.

Three-dimensional organization of DNA chains in complexes with dendrimers was found to result in DNA condensation through which the dendrimer-bound DNA chains aggregated significantly to form ordered structures. Safinya and colleagues performed an x-ray study of DNA complexes with G4 and G5 dendrimers [111]. The particular interest to study these generations was caused by the fact that G4 and G5 have intermediate size between low-molecular DNA condensing agents, by which DNA is compacted into bundles with hexagonal symmetry, and histones, which form ‘beads-on-a string’ structures on DNA. It was found that DNA–dendrimer complexes are columnar mesophases consisting of arrays of DNA ‘rods’ intercalated with dendrimers. The authors found a competition between square and hexagonal symmetry for the G4 complexes as a result of competition between long-range electrostatic cohesion and short-range electrostatic adhesion by counterion release. Hexagonal symmetry appeared under conditions of low and high loading ratios of DNA by dendrimers and square symmetry was found at ratios close to charge equivalence. Only square symmetry has been observed for the G5 dendrimer. This difference again emphasizes the change in DNA compaction mechanism from like-charge attraction between DNA chain segments to adsorption of DNA on charged surfaces, which leads to the disturbance of hexagonal packing typical for DNA compacted by multications.

Very recently [112], the dependence of DNA chain arrangement in complexes with G4 dendrimers on the DNA/dendrimer ratio was shown. Two types of mesomorphic structure characterized by different degrees of DNA ordering have been observed. At ratios of positive groups of dendrimer to negative groups of DNA between 2 and 4, the DNA–dendrimer complex exhibited a condensed nematic phase with short-range positional order of DNA chains (figure 10). DNA networks formed by the square columnar cells became less defective at larger ratios. Perfect networks consisting of DNA chains packed into a long-range ordered square lattice were formed at 4.0 ratio.

## 7. DNA compaction with nanoparticles

Recently, nanoparticles have become available from commercial sources and this initiated intensive studies on DNA interaction with nanoscale spherical objects. As we already mentioned, as a class of DNA compaction agents, nanoparticles fill the dimension gap between

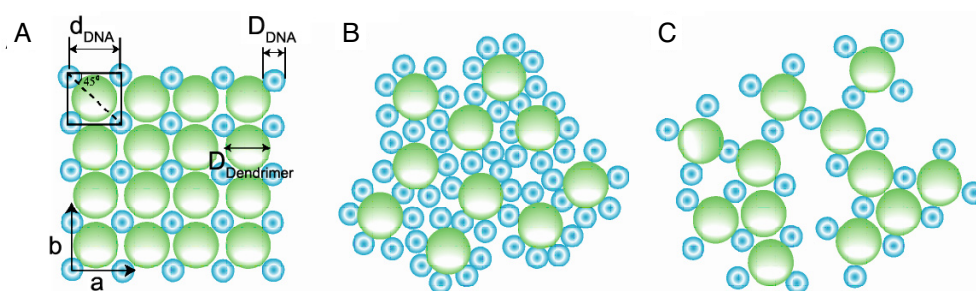


**Figure 10.** Schematic illustrations of the DNA packing. (A) Square columnar phase with  $d_{\text{DNA}^s} = 2^{-1/2}(D_{\text{dendrimer}} + D_{\text{DNA}})$ . (B) A nematic phase with the dendrimer molecules surrounded by the maximum number of DNA chains to maximize the charge matching for DNA. (C) A nematic phase containing defective DNA networks built up by irregularly packed square columnar cells. The diameter of the cross section of DNA and that of the dendrimer were drawn according to their actual relative size, namely, the diameter of DNA,  $D_{\text{DNA}} = 2.0$  nm, and  $D_{\text{dendrimer}} = 4.0$  nm =  $2D_{\text{DNA}}$ . Reproduced with permission from Liu *et al* [112]. Copyright 2005 American Chemical Society.

low-molecular chemicals and large cationic surfaces, and they provide an opportunity to vary the size of the nanotemplate from very tiny objects such as nanoclusters or quantum dots with sizes below 1 nm to very large nanoparticles of any desirable diameters up to microns and higher. Such nanoparticles are made of metal (usually, noble metal), semiconductors (such as CdS), silica or polymers. General patterns of DNA interaction with nanoparticles are not expected to differ much from the studies with dendrimers and are determined by the possibility or impossibility for the DNA chain to wrap a particle under certain solution conditions and nanoparticle surface curvature. What is probably new and advantageous in using nanoparticles compared to dendrimers is the opportunity to study DNA interaction with a fairly broad range of nanotemplate sizes and to decrease the mobility of surface charges.

As we discussed earlier, it is interesting to know the minimal size of nanoparticles at which DNA starts to wrap around nanospheres. It was shown that DNA cannot wrap around small gold cationically modified nanoparticles (smaller than about 5 nm). Such a collecting scenario leads to the formation of nanowires as was demonstrated for 2 nm size gold nanoparticles [113]. In contrast, when the size of the nanoparticles is about 30 nm, AFM measurement of free DNA chain before and after DNA complexation with nanoparticles showed that DNA makes on average a single wrap around such nanoparticles [114]. At a very high nanoparticle/DNA ratio, the wrapped species interconnect and form network structures. Therefore the reported appearance of a wrapping mechanism with respect to nanotemplate size is similar to the case of dendrimers as well as histone proteins, suggesting that the boundary between wrapping and collecting scenarios when nanoparticle size is about 5–10 nm (salt-containing solutions). In related investigations on polyelectrolytes, it was found that environmental conditions are important for interaction between nanoparticles and polyelectrolytes: very small gold nanoparticles with particle diameters down to 10 nm were successfully coated by a cationic agent only at finite, non-zero salt concentrations [115, 116]. In studies on correlation between DNA curvature and the size of nanoparticles there was found the shape-selective binding of oligonucleotides to neutral and cationic nanoparticles, in which intrinsically curved DNAs adsorbed more strongly to the curved nanoparticle surface [117, 118].

Keren and colleagues studied the phase behaviour of a system containing long DNA molecules and 16 nm positively charged gold colloids [119]. They established the phase diagram (figure 11) as a function of DNA/nanoparticle ratio at a fixed number of DNA bases

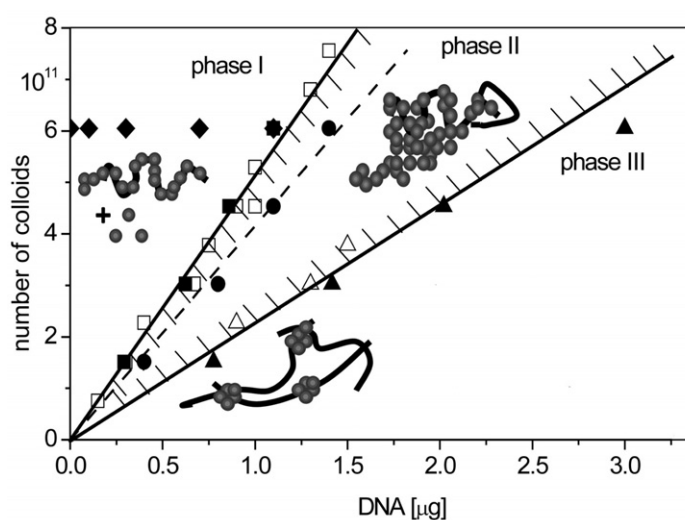


**Figure 11.** Phase diagram of colloid–DNA complexation as a function of DNA and colloid ratio. Phase boundaries are determined both by linear extrapolation of the reaction rate in phase II (e.g., inset) averaged over the first 6 min to zero reaction rate (solid symbols) and by sedimentation after 14 h (open symbols). The microscopic content of the three phases is plotted schematically. Phase I consists of generic nucleocolloid fibres in coexistence with free colloids. Phase II comprises large nucleocolloid clusters with some bare DNA segments and molecules. Phase III comprises small colloidal clusters localized on extensive DNA networks. Reproduced with permission from Keren *et al* [119]. Copyright 2002 American Physics Society.

per colloid, on which three phases can be defined. The fibre-shaped complex was observed in the presence of excess of gold colloids and such a phase (phase I) contains small clusters on DNA and free colloids. When the ratio between colloids and DNA approaches stoichiometry, the system undergoes a sharp coagulation transition and phase II comprises large clusters, thousands of colloids each, and no free colloids. The system is restabilized at higher DNA concentrations through localization of small colloid clusters on extensive DNA networks (phase III).

The adsorption of calf thymus DNA on 4.5 nm nanoparticles of Cd(II)-rich CdS was examined by photoluminescence spectroscopy as a function of temperature [120]. The obtained van't Hoff plot suggests that the driving force for DNA adsorption is entropy, and the enthalpic contribution to DNA–surface binding is slightly unfavourable. A likely source of the increase in entropy upon binding is the release of solvent and/or counterions from the interface, analogous to what has been observed for nonspecific protein–DNA interactions.

Our recent study made clear DNA compaction scenarios by cationic nanoparticles of sizes 10, 15, 40, and 100 nm [121]. It was shown that DNA chain compaction with cationic nanoscale templates is a stepwise and progressive process at the level of single DNA chains in contrast to the all-or-none DNA chain compaction mechanism realized in DNA compaction by multivalent cations. DNA compaction by nanoparticles leads to the formation of well-defined complexes (figure 12(B)) with a certain number of nanoparticles per DNA chain which is a function of physico-chemical parameters of the system such as DNA chain rigidity, nanoparticle size and charge, and salt concentration. Intermediated complexes are the analogues of ‘beads-on-a-string’ structures having unfolded and compact DNA chains in the same DNA molecule; however, together with individual particles on a DNA chain (figure 12(A)) we frequently observed clusters of nanoparticles bound to DNA separated by strings of unfolded parts of



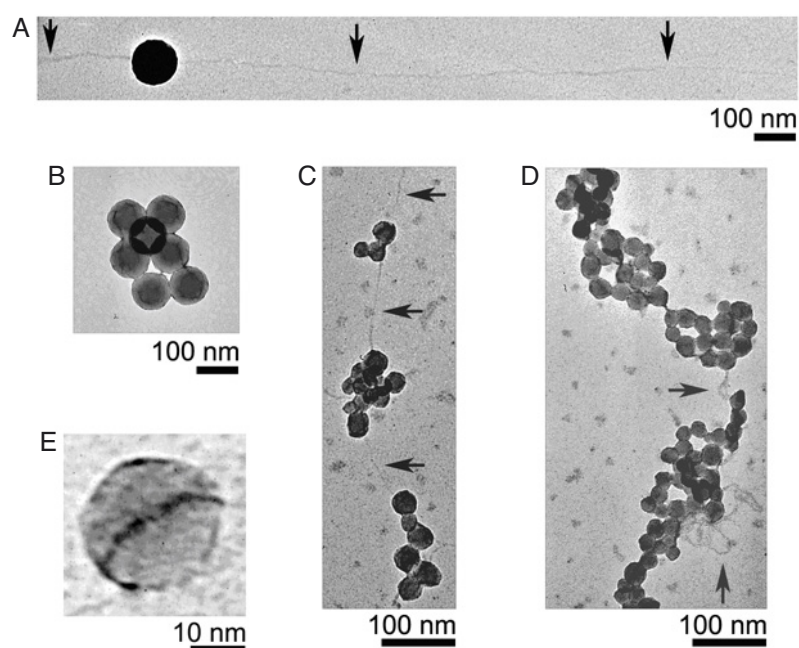


**Figure 12.** Transmission electron microscopy (TEM) pictures obtained at an acceleration voltage of 100 kV. Parts of unfolded, free, single DNA chain are indicated by arrows. (A) About 100 nm nanoparticle complexed along a single DNA chain. (B) Fully compact state of a single DNA chain complexed with 100 nm nanoparticles. (C) Part of a typical intermediate state of a single DNA chain in the presence of about 15 nm size nanoparticles. (D) Same as C at a higher nanoparticle concentration. (E) Close-up of about 20 nm nanoparticle complexed with DNA. The contrasted line (2 nm width) on the nanoparticle is attributed to the adsorbed DNA chain. Reproduced with permission from Zinchenko *et al* [121]. Copyright 2005 American Physics Society.

DNA (figures 12(C) and (D)). Several large 100 nm particles are incorporated into the compact complex with one T4 DNA molecular chain of 57  $\mu\text{m}$  length (here, the term ‘compact DNA’ means that at a certain concentration of nanoparticles no free chain of DNA is left) as shown in figure 12(B), while hundreds (15 nm) and even thousands (10 nm) of smaller nanoparticles are necessary to compact one DNA chain into the final condensate. Different ways of interaction can be distinguished based on the estimation of the adsorbed amount of DNA per particle (obtained from TEM observations) and calculations based on the geometry and charge parameters of the DNA and nanoparticles. These estimations define the free adsorption scenario for 100 and 40 nm nanoparticles, the wrapping scenario for 15 nm nanoparticles, and the collection scenario for the smallest 10 nm nanospheres. TEM observations allow the identification of the local DNA chain arrangement on the nanoparticle surface. For example, in figure 12(E) it can be seen how a DNA chain (2 nm width) wraps an about 20 nm cationic nanosphere around the equator line to minimize the bending energy.

Quantitative analysis of the charge ratio between the DNA phosphate and the nanoparticles’ positive charges, at which minimal value the complete DNA compaction (no free chain) occurs, provides several important conclusions. At optimal salt concentrations (0.1–0.5 M), the number of large nanoparticles (100 and 40 nm) required for DNA compaction is smaller than is required for stoichiometric DNA charge neutralization and suggests overcharging of nanoparticles by DNA. There is almost no difference between 100 and

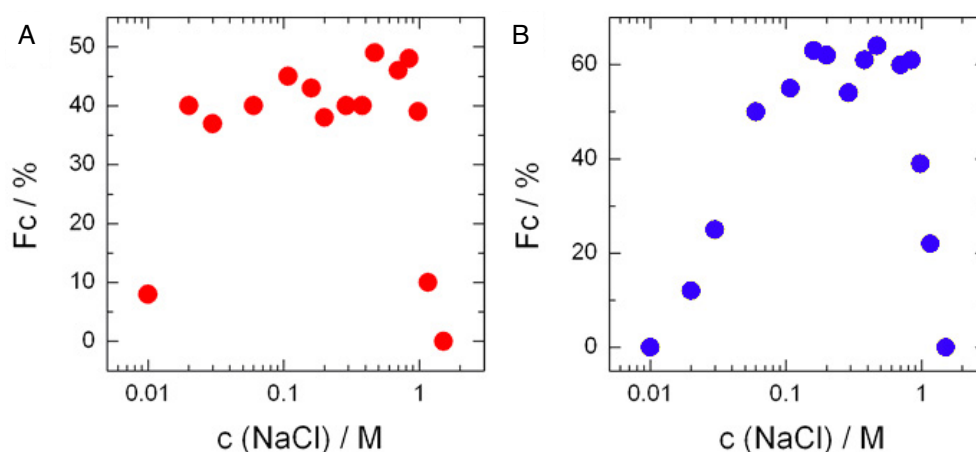


**Figure 13.** Salt effect on DNA compaction efficiency of nanoparticles. Percentage ( $F_c$ ) of individual DNA chains in the fully compact state (i.e. when all the length of DNA chain is adsorbed on particles) as a function of the salt concentration at a fixed concentration of about 100 nm (A) and about 40 nm (B) nanoparticles. Solutions with different concentrations of salt were prepared prior to adding the nanoparticles.

40 nm particles in terms of surface charge efficiency for DNA compaction in all the range of NaCl concentrations except very low salt conditions (below 0.01 M), probably due to the discrimination between 100 and 40 nm particles caused by large value of DNA persistent length (about 60 nm). On the other hand, to compact DNA by smaller nanoparticles (15 and 10 nm) the concentration of nanoparticles should be much higher than needed for charge equivalence between the DNA and the nanoparticles, but the maximum of compaction activity at intermediate salt conditions is nevertheless preserved.

Next, we have studied the effect of salt on DNA interaction with nanoparticles at fixed nanoparticle concentration. It was shown that the compaction efficiency of nanoparticles has a maximum at intermediate, close to physiological, salt concentrations, as illustrated in figure 13. In other words, at fixed concentration of nanoparticles, the conformation of a single DNA chain can be changed from unfolded into compact only by changing the salt concentration. The decrease in nanoparticle compaction activity when we move into the low salt region (i.e. decrease of compact DNA population) is explained by the increase of DNA chain bending energy cost to realize all ionic contacts with nanoparticles (especially important for smaller nanoparticles) and by increased repulsions between highly charged DNA cylinders adsorbed on the nanoparticle surface (especially important for larger nanoparticles). On the other hand, the decrease of nanoparticle compaction activity at high concentrations of salt was due to screening of electrostatic interactions between the DNA chain and the nanoparticles. Such a general tendency was observed for all particle sizes from 10 to 100 nm; however, we found that with a decrease of nanoparticle size the increase of nanoparticle compaction activity (when we start from zero salt and increase the salt concentration) continues until higher salt concentration (cf cases of 100 and 40 nm nanoparticles in figure 13). If the nanoparticles are large, the drop of their compaction activity is steep and there is a long plateau at middle salt conditions, while in the case of very small nanoparticles such as 10 nm nanospheres, the plateau collapses into a clear peak at rather high salt concentrations (data not shown).

To conclude this part we would like to mention briefly another spherical nanostructure—fullerene. Fullerene is a carbon nanosphere with a diameter about 1 nm. The size of fullerene



is very small and is comparable with the dimension of dendrimers of G2–G3 generations. Therefore, for fullerene interaction with DNA only the scenario of collecting is expected. Experimental investigations on DNA compaction with cationically modified fullerenes made it clear that, in contrast to the second generation of cationic dendrimers, the toroidal structure of DNA is not preserved and DNA is compacted into globules [122]. This can be due to the fact that fullerene is more rigid than a dendrimer and this prevents intrinsic DNA chain toroidal organization upon compaction such as during compaction with multications. Finally, we would like to note the interesting fact that although DNA adsorption on surfaces is predominantly electrostatic, even disfavoured electrostatics can be overcome by specific interactions. As an example, it was demonstrated that single-stranded DNA is continuously adsorbed on the negatively charged surface of DNA-coated nanoparticles due to complementary guanine–cytosine interactions [123].

## 8. Theoretical and experimental studies on DNA interaction with nanotubes

Spherical nanostructures have corresponding elongated analogues: the carbon nanotube is actually an elongated form of fullerene, nanorods are elongated nanoparticles, and dendrimers have elongated representatives such as dendronized polymers. In fact, experimental reports about double-stranded DNA interaction with tubular nanostructures is almost unavailable at the present moment; therefore, in this part we describe both cases of single- and double-stranded DNAs to show the progress in this area.

Kunze and Nenz studied complexation between a charged cylinder and a semi-flexible chain using linear Debye–Hückel theory, and they discuss two possible scenarios of interaction: adsorption of polyelectrolyte in a straight form or helical adsorption [124]. According to the phase diagram obtained, straight morphology of complexation is favoured for more rigid chains and for higher salt concentrations. Although they discussed this complexation as a model of peptide chain interaction with the DNA cylinder, it can be also applicable to describe the adsorption of DNA on nanocylinders such as nanotubes and nanorods. Extending the results of Kunze and Netz, Cherstvy and Winkler calculated the electrostatic potential and energy of the helical (cylinder–chain) complex using linear Poisson–Boltzmann theory. They found that sufficiently flexible chains preferred to wrap around the cylinder in a helical manner, when their charge density was smaller than that of the cylinder [125]. They studied the dependence of the pitch (distance between adjacent DNA wraps on the cylinder) on various parameters by minimizing the electrostatic and bending energy of DNA. The results indicate that for larger concentrations of salt the optimal pitch of the semi-flexible chain helix around the cylinder increases since the electrostatic interaction is screened. On the other hand, with an increase in the cylinder radius, the corresponding electrostatic energy decreases for fixed linear charge densities, leading to higher values of the helical pitch, although the bending energy decreases, and to a weaker charge neutralization of the cylinder by wrapped strings. With decreasing linear charge densities, the value of the helical pitch increases more rapidly with the persistence length.

By application of the Poisson–Boltzmann equation, the electrostatic potential, electrostatic free energies, entropic free energies and distribution of counterions were determined for a series of DNA–dendronized polymer complexes with different DNA pitches [126]. The results of this study show that in a series of conformations at constant ionic strength, the electrostatic free energies and entropic free energies first decreased sharply and then smoothly increased with the increase in DNA pitch size. The authors suggest that this happens due to the increasing charge density of the positive mobile ions and decreasing charge density of the negative mobile ions around the DNA–dendronized polymer nanocluster.

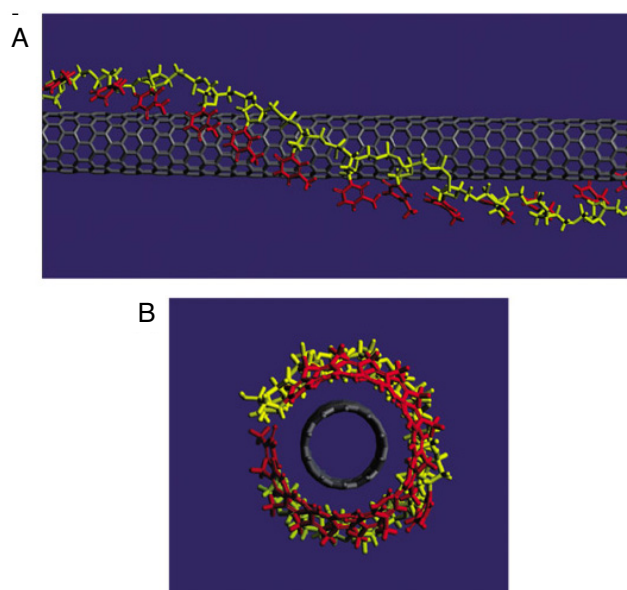


**Figure 14.** Binding model of a carbon nanotube wrapped by a poly(T) sequence. (A) The right-handed helical structure shown here is one of several binding structures found, including left-handed helices and linearly adsorbed structures. In all cases, the bases orient to stack with the surface of the nanotube, and extend away from the sugar–phosphate backbone. (B) The DNA wraps to provide a tube within which the carbon nanotube can reside, hence converting it into a water-soluble object. Reproduced with permission from Zheng *et al* [128]. Copyright 2003 Nature Publishing Group.

Most theoretical investigations show that in the case of a charged cylinder, the charge of adsorbed polymer is also larger than is necessary for cylinder charge neutralization, as is similarly found for DNA–nanosphere interaction [63]. Park and colleagues studied the overcharging of a negatively charged semi-flexible chain and a positively charged rigid cylinder [124, 82], based on the classical mean-field Poisson–Boltzmann treatment of electrostatic interactions, and found that complexation of both flexible and rigid oppositely charged polyelectrolytes should lead to overcharging of the complex due to entropic effects, related to the counterion release mechanism. In contrast to that, recent theoretical studies of Cherstvy and Winkler suggest that neutral and undercharged complexes are preferred [125].

The experimental data about DNA interaction with nanoscale templates are limited by a few papers. In spite of almost no fundamental experimental works in this research field, utilization of DNA wrapped on nanotubes as nanoscale transistors has been suggested quite early, and this area is now quickly developing. Single wall carbon nanotubes (SWCNs) were mainly studied as nanoscale templates for DNA interaction. The cylindrical morphology of nanotubes allows polymer to wrap around the nanotube to form a helix, which is characterized by a pitch between adjacent DNA chains. Interestingly, interaction of a carbon nanotube with DNA can be realized even without electrostatic binding through  $\pi$ -bonding between DNA and the nanotube [127]. Molecular modelling experiments show that single-stranded DNA binds to carbon nanotubes through  $\pi$ -stacking, resulting in helical wrapping to the surface as shown in figure 14 [128]. Driven by  $\pi$ -interactions, solubilization of carbon nanotubes in water through binding with DNA has been repeatedly demonstrated [127, 129].

AFM measurements show that short d(GT)<sub>n</sub>-CNT hybrids have a uniform periodic structure with a regular pitch of 18 nm [130]. Very recently, the wrapping of a long genomic

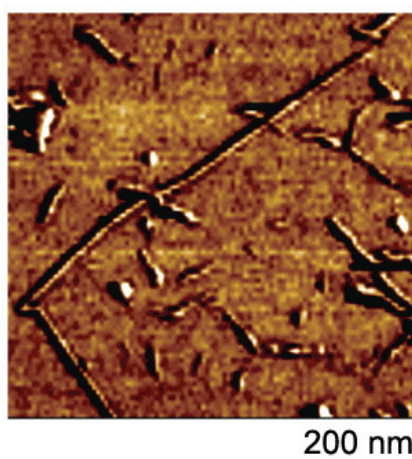


**Figure 15.** Phase AFM image of several single-stranded DNA-wrapped carbon nanotubes with regular pitches. Reproduced with permission from Gigliotti *et al* [131]. Copyright 2006 American Chemical Society.

single-stranded DNA has been investigated by AFM and it was demonstrated that the DNA chain wraps periodically around the nanotube [131]. A microscopic picture of a DNA–nanotube complex is shown in figure 15, where the periodic wrapping can be clearly seen. *Double*-stranded DNA wrapping around nanotube has never been observed. The cylindrical morphology of the polycation can be realized by a synthetic approach similar to dendrimers, where the polymer chain is propagated into a perpendicular direction [132]. The model of DNA interaction with a charged dendronized polymer is shown in figure 16, according to which the polyelectrolyte with the smaller linear charge density (DNA) is wrapped around the more highly charged dendronized polymer. Two representatives of dendronized polymers were studied, having different thickness about 1.6 and 3.3 nm, and it was shown that the interplay between the electrostatic energy and elastic energy defines both the overall charge of the complex and the different pitch sizes (16.3 and 27 nm, respectively) for the wrapped DNA. Both DNA complexes are overcharged by DNA, and the overcharging is higher for smaller-diameter cylinder.

Comparison of DNA interaction with spherical and cylindrical dendrimers indicates that stronger DNA complexes are formed with cylindrical dendrimers rather than with spherical one [106, 133].

## 9. Conclusions and perspectives

As has been already mentioned in the introduction, we are still at a very early stage of experimental modelling of systems where DNA is compacted on nanoscale three-dimensional templates. Therefore, the awaited progress in this field is dramatic and we expect that it is in the coming decade that we will observe new and exciting results in this area. Theoretical studies on this fundamental problem go far in advance of experimental modelling, and reading theoretical works published in recent years, one can mention that the experimental papers cited by the theoretical physicists are limited by a small number of separate experimental studies. Therefore, experimental results on DNA interaction with a large variety of nanoscale templates will be an important contribution to verify earlier theoretical predictions as well as to gain deeper insight into relevant biological problems. Another interesting and almost

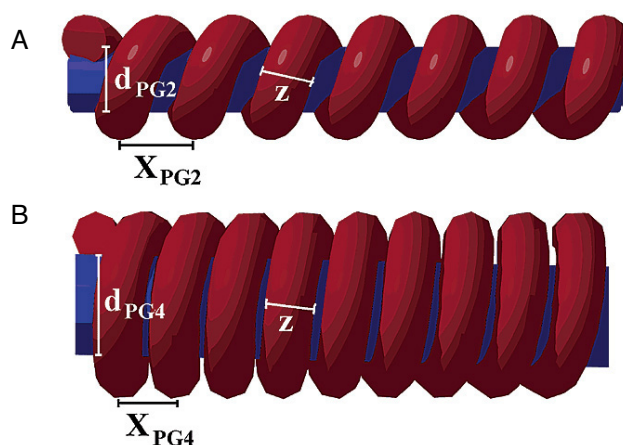


**Figure 16.** Models of the double-stranded DNA complex with dendronized polymers having different diameters. DNA wraps around the dendronized polymer of second (A) and fourth (B) generations, resulting in the formation of pitches. Reproduced with permission from Gössl *et al* [132]. Copyright 2002 American Chemical Society.

unexplored (both theoretically and experimentally) issue is the connection points between two mechanisms of DNA compaction, i.e. abrupt switch of DNA conformation (first-order phase transition) upon DNA compaction by multivalent cations and compaction of DNA with nanoscale objects (similar to the formation of the ‘beads-on-a-string’ structure and further packaging of chromatin). Between these two cases, interesting behaviour of the DNA chain during compaction can be expected. With the recent progress in the synthesis of nanoscale templates, elaboration of biomimetic systems where, for instance, nanoparticles play a role of proteins, is expected. Along with the fundamental importance of such structures, they will contribute invaluablely in the biotechnology field towards the construction of new vectors for DNA gene delivery.

### Acknowledgments

AAZ is grateful to Professor H Löwen for his kind invitation to write this review. The authors acknowledge collaboration with Dr D Baigl and Dr T Sakaue. Dr A Cherstvy is gratefully acknowledged for helpful communications. The authors are indebted to Professor K Yoshikawa and all members of his laboratory in Kyoto University for encouragements in studies on DNA compaction phenomena. This work is supported in part by ICORP Spatio-Temporal Order Project (JST).

### References

- [1] Livolant F 1991 *Physica A* **176** 117
- [2] Cerritelli M E, Cheng N, Rosenberg A H, McPherson C E, Booy F P and Steven A C 1997 *Cell* **91** 271
- [3] Schiessel H 2003 *J. Phys.: Condens. Matter* **15** R699
- [4] Grosberg A Yu and Khokhlov A R 1994 *Statistical Physics of Macromolecules* (New York: American Institute of Physics)
- [5] Zauner W, Ogris M and Wagner E 1998 *Adv. Drug Deliv. Rev.* **30** 97
- [6] Bloomfield V A 1996 *Curr. Opin. Struct. Biol.* **6** 334
- [7] Hud N V and Vilfan I D 2005 *Ann. Rev. Biophys. Biomol. Struct.* **34** 295

- [8] Yoshikawa K and Yoshikawa Y 2002 *Pharmaceutical Perspectives of Nucleic Acid-Based Therapeutics* (London: Taylor and Francis) p 137
- [9] Zinchenko A A, Baigl D and Yoshikawa K 2006 *Polymeric Nanostructures and their Applications* ed H S Nalwa (Stevenson Ranch (CA), USA: American Scientific)
- [10] Joanny J-F, Castelnovo M and Netz R 2000 *J. Phys.: Condens. Matter* **12** A1
- [11] Grosberg A Yu, Nguyen T T and Shklovskii B I 2002 *Rev. Mod. Phys.* **74** 329
- [12] Baigl D and Yoshikawa K 2005 *Biophys. J.* **88** 3486
- [13] North A C T and Rich A 1961 *Nature* **191** 1242
- [14] Tsodikov O V, Saecker R M, Melcher S E, Levandoski M M, Frank D E, Capp M W and Record MT Jr 1999 *J. Mol. Biol.* **294** 639
- [15] Kampranis S C, Bates A D and Maxwell A 1999 *Proc Natl Acad. Sci. USA* **96** 8414
- [16] Verhoeven E E, Wyman C, Moolenaar G F, Hoeymakers J H and Goosen N 2001 *EMBO J.* **20** 601
- [17] Baumann C G, Smith S B, Bloomfield V A and Bustamante C 1997 *Proc. Natl Acad. Sci. USA* **94** 6185
- [18] Saecker R M and Record MT Jr 2002 *Curr. Opin. Struct. Biol.* **12** 311
- [19] van Holde K E 1988 *Chromatin (Springer Series in Molecular Biology)* (New York: Springer)
- [20] Tsanev R, Russev G, Pashev I and Zlatanova J 1992 *Replication and Transcription of Chromatin* vol 269 (Boca Raton, FL: CRC Press)
- [21] Wolffe A P 1998 *Chromatin: Structure and Function* (New York: Academic)
- [22] Turner B M 2002 *Chromatin and Gene Regulation: Mechanisms in Epigenetics* (Oxford: Blackwell Science)
- [23] Kornberg R D 1977 *Annu. Rev. Biochem.* **46** 931
- [24] Oudet P, Gross-Bellard M and Chambon P 1975 *Cell* **4** 281
- [25] Luger K, Mader A W, Richmond R K, Sargent D F and Richmond T J 1997 *Nature* **389** 251
- [26] Klug A, Finch J T and Richmond T J 1985 *Science* **229** 1109
- [27] Richmond T J, Finch J T, Rushton B, Rhodes D and Klug A 1984 *Nature* **311** 532
- [28] Davey C A, Sargent D F, Luger K, Maeder A W and Richmond T J 2002 *J. Mol. Biol.* **319** 1097
- [29] Arents G and Moudrianakis E N 1993 *Proc. Natl Acad. Sci. USA* **90** 10489
- [30] van Holde K and Zlatanova J 1999 *Bioessays* **21** 776
- [31] Harp J M, Hanson B L, Timm D E and Bunick G J 2000 *Acta Crystallogr. D* **56** 1513
- [32] McGhee J D and Felsenfeld G 1980 *Nucl. Acids Res.* **8** 2751
- [33] Thoma F, Koller T and Klug A 1979 *J. Cell. Biol.* **83** 403
- [34] Thoma F and Koller Th 1981 *J. Mol. Biol.* **149** 709
- [35] Finch J T and Klug A 1976 *Proc. Natl Acad. Sci. USA* **73** 1897
- [36] Woodcock C L, Grigoryev S A, Horowitz R A and Whitaker N 1993 *Proc. Natl Acad. Sci. USA* **90** 9021
- [37] Daban J-R 1999 *Biochemistry* **39** 3861 and references therein
- [38] Thoma F and Koller T 1977 *Cell* **12** 101
- [39] Mergell B, Everaers R and Schiessel H 2004 *Phys. Rev. E* **70** 011915
- [40] Hizume K, Yoshimura S H and Takeyasu K 2005 *Biochemistry* **44** 12978
- [41] Nakai T, Hizume K, Yoshimura S, Takeyasu K and Yoshikawa K 2005 *Europhys. Lett.* **69** 1024
- [42] Leuba S H, Zlatanova J, Karymov M A, Bash R, Liu Y-Z, Lohr D, Harrington R E and Lindsay S M 2000 *Single Mol.* **1** 185
- [43] Rief M, Gautel M, Oesterhelt F, Fernandez J M and Gaub H E 1997 *Science* **276** 1109
- [44] Oberhauser A F, Marszalek P E, Erickson H P and Fernandez J M 1998 *Nature* **393** 181
- [45] Zlatanova J and Leuba S H 2003 *J. Mol. Biol.* **331** 1
- [46] Polach K J and Widom J J 1995 *Mol. Biol.* **254** 130
- [47] Kulic I M and Schiessel H 2004 *Phys. Rev. Lett.* **92** 228101
- [48] Gottesfeld J M, Belitsky J M, Melander C, Dervan P B and Luger K 2002 *J. Mol. Biol.* **321** 249
- [49] Kulic I M and Schiessel H 2003 *Phys. Rev. Lett.* **91** 148103
- [50] Becker P B 2002 *EMBO J.* **21** 4749
- [51] Pennings S, Meersseman G and Bradbury E M 1994 *Proc. Natl Acad. Sci.* **91** 10275
- [52] Champoux J J 2001 *Annu. Rev. Biochem.* **70** 369
- [53] Liu L F and Wang J C 1978 *Proc. Natl Acad. Sci. USA* **75** 2098
- [54] Maxwell A, Gellert M and McTurk P 1989 *Highlights Mod. Biochem.* **1** 97
- [55] Reece R J and Maxwell A 1991 *Crit. Rev. Biochem. Mol. Biol.* **26** 335
- [56] Heddle J G, Mittelheiser S, Maxwell A and Thomson N H 2004 *J. Mol. Biol.* **337** 597
- [57] Bednar J, Horowitz R A, Grigoryev S A, Carruthers L M, Hansen J C, Koster A J and Woodcock C L 1998 *Proc. Natl Acad. Sci. USA* **95** 14173
- [58] Martino J A, Katritch V and Olson W K 1999 *Structure* **7** 1009
- [59] Schiessel H, Gelbart W M and Bruinsma R F 2001 *Biophys. J.* **80** 1940



- [60] Ben-Haim E, Lesne A and Victor J-M 2001 *Phys. Rev. E* **64** 051921
- [61] Clark D J and Kimura T 1990 *J. Mol. Biol.* **211** 883
- [62] Beard D A and Schlick T 2001 *Structure* **9** 105
- [63] Netz R R and Joanny J-F 1999 *Macromolecules* **32** 9026
- [64] Kunze K-K and Netz R R 2002 *Phys. Rev. E* **66** 011918
- [65] Sakaue T and Löwen H 2004 *Phys. Rev. E* **70** 021801
- [66] Sakaue T, Yoshikawa K S, Yoshimura H and Takeyasu K 2001 *Phys. Rev. Lett.* **87** 078105
- [67] Schiessel H 2003 *Macromolecules* **36** 3424
- [68] Schiessel H, Rudnick J, Bruinsma R and Gelbart W M 2000 *Europhys. Lett.* **51** 237
- [69] Akinchina A and Linse P 2002 *Macromolecules* **35** 5183
- [70] Li W, Dou S-X and Wang P-Y 2005 *J. Theor. Biol.* **235** 365
- [71] Boroudjerdi H and Netz R R 2003 *Europhys. Lett.* **64** 413
- [72] Mühlbacher F, Holm C and Schiessel H 2006 *Europhys. Lett.* **73** 135
- [73] Boroudjerdi H and Netz R R 2005 *J. Phys.: Condens. Matter* **17** S1137
- [74] Mateescu E M, Jeppesen C and Pincus F 1999 *Europhys. Lett.* **46** 493
- [75] Nguyen T T and Shklovskii B I 2001 *Physica A* **293** 324
- [76] Nguyen T T and Shklovskii B I 2001 *J. Chem. Phys.* **114** 5905
- [77] Schiessel H, Bruinsma R F and Gelbart W M 2001 *J. Chem. Phys.* **115** 7245
- [78] Decher G 1997 *Science* **277** 1232
- [79] Caruso F, Lichterfeld H, Donath E and Möhwald H 1999 *Macromolecules* **32** 2317
- [80] Bruinsma R 1998 *Eur. Phys. J. B* **4** 75
- [81] Cherstvy A G and Winkler R G 2005 *J. Phys. Chem. B* **109** 2962
- [82] Park S Y, Bruinsma R F and Gelbart W M 1999 *Europhys. Lett.* **46** 454
- [83] Manning G S 2003 *J. Am. Chem. Soc.* **125** 15087
- [84] Wallin T and Linse P 1996 *Langmuir* **12** 305
- [85] Wallin T and Linse P 1997 *J. Phys. Chem.* **101** 5506
- [86] Chodanowski P and Stoll S 2001 *Macromolecules* **34** 2320
- [87] Jonsson M and Linse P 2001 *J. Chem. Phys.* **115** 3406
- [88] Jonsson M and Linse P 2001 *J. Chem. Phys.* **115** 10975
- [89] Wallin T and Linse P 1996 *J. Phys. Chem.* **100** 17873
- [90] Dubin P L, Curran M E and Hua J 1990 *Langmuir* **6** 707
- [91] McQuigg D W, Kaplan J I and Dubin P L 1992 *J. Phys. Chem.* **96** 1973
- [92] Huebner S, Battersby B J, Grimm R and Cevc G 1999 *Biophys. J.* **76** 3158
- [93] Clausen-Schaumann H and Gaub H E 1999 *Langmuir* **15** 8246
- [94] Fang Y and Yang J 1997 *Phys. Chem. B* **110** 3453
- [95] Koltover I, Wagner K and Safinya C R 2000 *Proc. Natl Acad. Sci. USA* **97** 14046
- [96] Pitard B, Aguerre O, Airiau M, Lachage's A M, Boukhnikachvili T, Byk G, Dubertret C, Herviou C, Scherman D, Mayaux J F and Crouzet J 1997 *Proc. Natl Acad. Sci. USA* **94** 14412
- [97] Rädler J O, Koltover I, Salditt T and Safinya C R 1997 *Science* **275** 810
- [98] Rädler J O, Koltover I, Jamieson A, Salditt T and Safinya C R 1998 *Langmuir* **14** 4272
- [99] Lasic D D, Strey H, Stuart M C A, Podgornik R and Frederik P M 1997 *J. Am. Chem. Soc.* **119** 832
- [100] Koltover I, Salditt T and Safinya C R 1999 *Biophys. J.* **77** 915
- [101] Gershon H, Ghirlando R, Guttman S B and Minsky A 1993 *Biochemistry* **32** 7143
- [102] Koltover I, Salditt T, Rädler J O and Safinya C R 1998 *Science* **281** 78
- [103] Liang H, Angelini T E, Ho J, Braun P V and Wong G C L 2003 *J. Am. Chem. Soc.* **125** 11786
- [104] Frechet J M J 1994 *Science* **263** 1710
- [105] Ottaviani M F, Furini F, Casini A, Turro N J, Jockusch S, Tomalia D A and Messori L 2000 *Macromolecules* **33** 7842
- [106] Chen W, Turro N J and Tomalia D A 2000 *Langmuir* **16** 15
- [107] Kabanov V A, Sergeyev V G, Pyshkina O A, Zinchenko A A, Zezin A B, Joosten J G H, Brackman J and Yoshikawa K 2000 *Macromolecules* **33** 9587
- [108] Bielinska A U, Kukowska-Latallo J F and Baker J R Jr 1997 *Biochim. Biophys. Acta* **1353** 180
- [109] Abdelhady H G 2004 *PhD Thesis* The University of Nottingham, England
- [110] Tang M X, Redmann C T and Szoka F C Jr 1996 *Bioconjug. Chem.* **7** 703
- [111] Evans H M, Ahmad A, Ewert K, Pfohl T, Martin-Herranz A, Bruinsma R F and Safinya C R 2003 *Phys. Rev. Lett.* **91** 075501
- [112] Liu Y C, Chen H L, Su C J, Lin H K, Liu W L and Jeng U S 2005 *Macromolecules* **38** 9434

- [113] Kumar A, Pattarkine M, Bhadbhade M, Mandale A B, Ganesh K N, Datar S S, Dharmadhikari C V and Sastry M 2001 *Adv. Mater.* **13** 341
- [114] Ganguli M, Babu J V and Maiti S 2004 *Langmuir* **20** 5165
- [115] Gittins D I and Caruso F 2000 *Adv. Mater.* **12** 1947
- [116] Gittins D I and Caruso F 2001 *J. Phys. Chem. B* **105** 6846
- [117] Mahtab R, Rogers J P and Murphy C J 1995 *J. Am. Chem. Soc.* **117** 9099
- [118] Mahtab R, Rogers J P, Singleton C P and Murphy C J 1996 *J. Am. Chem. Soc.* **118** 7028
- [119] Keren K, Soen Y, Yoseph G B, Gilad R, Braun E, Sivan U and Talmon Y 2002 *Phys. Rev. Lett.* **89** 088103
- [120] Mahtab R, Harden H H and Murphy C J 2000 *J. Am. Chem. Soc.* **122** 14
- [121] Zinchenko A A, Yoshikawa K and Baigl D 2005 *Phys. Rev. Lett.* **95** 228101
- [122] Isobe H, Sugiyama S, Fukui K, Iwasawa Y and Nakamura E 2001 *Angew. Chem. Int. Edn* **40** 3364
- [123] Johnston A P R, Read E S and Caruso F 2005 *Nano Lett.* **5** 953
- [124] Kunze K K and Netz R R 2002 *Europhys. Lett.* **58** 299
- [125] Cherstvy A G and Winkler R G 2004 *J. Chem. Phys.* **120** 9394
- [126] Nikakhtar A, Nasehzadeh A, Naghibi-Beidokhti H and Mansoori G A 2005 *J. Comput. Theor. Nanosci.* **2** 1
- [127] Nakashima N, Okuzono S, Murakami H, Nakai T and Yoshikawa K 2003 *Chem. Lett.* **132** 456
- [128] Zheng M, Jagota A, Semke E D, Diner B A, Mclean R S, Lustig S R, Richardson R E and Tassi N G 2003 *Nat. Mater.* **2** 338
- [129] Hu C, Zhang Y, Bao G, Zhang Y, Liu M and Wang Z L 2005 *J. Phys. Chem. B* **109** 20072
- [130] Zheng M, Jagota A, Strano M S, Santos A P, Barone P, Chou S G, Diner B A, Dresselhaus M S, Mclean R S, Onoa G B, Samsonidze G G, Semke E D, Usrey M and Walls D J 2003 *Science* **302** 1545
- [131] Gigliotti B, Sakizzie B, Bethune D S, Shelby R M and Cha J N 2006 *Nano Lett.* **6** 159
- [132] Gössl I, Shu L, Schlüter A D and Rabe J P 2002 *J. Am. Chem. Soc.* **124** 6860
- [133] Gössl I, Shu L, Schlüter A D and Rabe J P 2002 *Single Mol.* **3** 315
- [134] Richmond T J and Davey C A 2003 *Nature* **423** 145
- [135] Kunze K K and Netz R R 2000 *Phys. Rev. Lett.* **85** 4389